SMJ Singapore Medical Journal

Radiographic features of COVID-19 based on an initial cohort of 96 patients in Singapore

Hau Wei Khoo[1], MD, FRCR, Terrence Chi Hong Hui[1,*], MBBS, FRCR, Salahudeen Mohamed Haja Mohideen[2,*], MBBS, FRCR, Yeong Shyan Lee[1], MBBCh, FRCR, Charlene Jin Yee Liew[3,4], MBBS, FRCR, Shawn Shi Xian Kok[5], MBBS, FRCR, Barnaby Edward Young[6,7], MB BChir, MRCP, Sean Wei Xiang Ong[6,7], MBBS, Shirin Kalimuddin[4,8], MBBS, MPH, Seow Yen Tan[9], MBBS, MRCP, Jiashen Loh[10], MBBS, MRCP, Lai Peng Chan[2,11], MBBS, FRCR, Angeline Choo Choo Poh[3], MBBS, FRCR, Steven Bak Siew Wong[5], MBChB, MMed, Yee-Sin Leo[6,7,11,12,13], MPH, FRCP, David Chien Lye[6,7,11,13], FRACP, FRCP, Gregory Jon Leng Kaw[1], MBBS, FRCR, Cher Heng Tan[1,13], MBBS, FRCR

[1]Department of Diagnostic Radiology, Tan Tock Seng Hospital, [2]Department of Diagnostic Radiology, Singapore General Hospital, [3]Department of Diagnostic Radiology, Changi General Hospital, [4]Duke-NUS Medical School, [5]Department of Radiology, Sengkang General Hospital, [6]National Centre for Infectious Diseases, [7]Department of Infectious Diseases, Tan Tock Seng Hospital, [8]Department of Infectious Diseases, Singapore General Hospital, [9]Department of Infectious Diseases, Changi General Hospital, [10]Department of Infectious Diseases, Sengkang General Hospital, [11]Yong Loo Lin School of Medicine, [12]Saw Swee Hock School of Public Health, National University of Singapore, [13]Lee Kong Chian School of Medicine, Nanyang Technological University, Singapore
*These authors contributed equally as second authors in this work.

Correspondence: Dr Cher Heng Tan, Senior Consultant, Department of Diagnostic Radiology, Tan Tock Seng Hospital, 11 Jalan Tan Tock Seng, Singapore 308433. cher_heng_tan@ttsh.com.sg

Singapore Med J 2020, 1–22
https://doi.org/10.11622/smedj.2020142
Published ahead of print: 21 September 2020

Online version can be found at
http://www.smj.org.sg/online-first

ABSTRACT

Introduction: Chest radiographs (CXR) are widely used for the screening and management of the coronavirus disease 2019 (COVID-19). This paper determinates the radiographic features of COVID-19 based on an initial national cohort of patients.

Methods: This is a retrospective review of swab-positive COVID-19 patients admitted to four different hospitals in Singapore between 22 January and 9 March 2020. Initial and follow-up CXR were reviewed by three experienced radiologists to identify the predominant pattern and distribution of lung parenchymal abnormalities.

Results: In total, 347 CXR of 96 patients were reviewed. Initial CXR were abnormal in 41 out of 96 patients (42.7%). The mean time from onset of symptoms to CXR abnormality was 5.3 (range 1–21) days. The predominant pattern of lung abnormality was ground-glass opacity on initial CXR (51.2%) and consolidation on follow-up CXR (51.0%). Multifocal bilateral abnormalities in mixed central and peripheral distribution were seen in 63.4% and 59.2% of abnormal initial and follow-up CXR, respectively. The lower zones were involved in 90.2% of the initial CXR and 93.9% of the follow-up CXR.

Conclusion: In a cohort of swab-positive patients, including those identified from contact tracing, we found the incidence of CXR abnormality to be lower than previously reported. The most common pattern was ground-glass opacity or consolidation, but mixed central and peripheral involvement was more common than peripheral involvement alone.

Keywords: chest radiographs, coronavirus disease 2019, SARS-CoV-2

INTRODUCTION

Coronaviruses are enveloped positive-sense RNA viruses known to cause upper and lower respiratory tract infections in addition to gastrointestinal, hepatic and neurologic diseases.[1-3] While most infections are mild, coronaviruses have emerged as an important pathogen since the severe acute respiratory syndrome (SARS) epidemic in 2002–2003. SARS was the first known coronavirus to cause severe respiratory illness in immunocompetent adults and has an overall mortality rate of 9.6%,[4] predominantly affecting the elderly aged above 60 years where the estimated mortality rate was as high as 43%–50%.[3] In 2012, the Middle East respiratory syndrome (MERS) emerged in Saudi Arabia with an even higher mortality rate of 37.1%.[5]

In December 2019, a team from the Chinese Centre for Disease Control and Prevention investigated an emerging cluster of patients with pneumonia of unknown aetiology in the city of Wuhan, Hubei Province, China.[6] The team subsequently isolated a novel coronavirus on 7 January 2020, which was later named as SARS-CoV-2.[7,8] This new virus represents the third virus of the *Coronaviridae* family to cause severe respiratory disease in the healthy population. Since then, the virus has spread worldwide and the World Health Organization (WHO) declared the outbreak to be a public health emergency of international concern on 30 January 2020. WHO subsequently named the disease ‘coronavirus disease 2019’ (COVID-19) on 11 February 2020. As the number of confirmed cases grew to more than 118,000 with more than 4,200 deaths worldwide, WHO declared the outbreak a pandemic on 11 March 2020.[9]

Although chest radiography (CXR) is less sensitive in detecting ground-glass opacities compared to computed tomography (CT),[10] it remains an essential initial radiological investigation in the screening and management of COVID-19 pneumonia. In Singapore, reverse-transcription polymerase chain reaction (RT-PCR) of respiratory samples is used as the standard

for confirmatory diagnosis of COVID-19 infection. CXR is utilised for the initial detection of radiographic apparent pneumonia and triaging of suspected cases due to its easy availability, instant diagnostic capability and low cost. Moreover, radiographic resolution of abnormalities has been used as an important criterion for discharging patients from hospital among other clinical parameters.[11] CXR promptly detects cases that are complicated by acute respiratory distress syndrome (ARDS), which warrants intensive care, including mechanical ventilation. Deterioration to ARDS generally indicates a poor prognosis – Chen et al found that 11 out of 17 (64.7%) patients with ARDS died of multiorgan failure,[12] while Zhu et al described a case of ARDS that showed worsening of diffuse consolidation on CXR performed on Days 8 and Day 11 of symptoms, and the patient passed away on Day 21 despite intensive care unit management.[6] Finally, CXR plays a crucial role in excluding other causes of hypoxia that are imminently treatable. For example, although not encountered in our series and considered a rare complication, a case of pneumothorax was reported by Chen et al on initial CXR.[12]

Despite the widespread use of CXR for managing COVID-19, there have been a limited number of studies analysing the imaging features of this imaging modality. In this article, we described the radiographic findings of COVID-19 pneumonia across a spectrum of swab-positive patients. In our discussion, we contrasted our findings for COVID-19 from reported features of other viral pneumonia, with attention to SARS and MERS, the two other lethal human coronavirus infections.

METHODS

Informed consent from study participants for this retrospective review study was waived by the Singapore Ministry of Health under the Infectious Diseases Act (Chapter 137). Between 22

January to 9 March 2020, 96 confirmed cases of COVID-19 admitted to four institutions in Singapore were included in this study. COVID-19 infection was confirmed by RT-PCR assay on two nasopharyngeal and throat swabs 24 hours apart at the National Public Health Laboratory. As little was known about the virulence of the pathogen at the onset of the pandemic, all patients were managed in negative pressure isolation rooms – 91 patients at the National Centre for Infectious Diseases, three at Singapore General Hospital, one at Changi General Hospital and one at Sengkang General Hospital. Patient demographics and clinical data were collected from electronic medical records.

Radiographic examinations were obtained using digital radiography equipment (Fluorospot Compact FD; Siemens, Erlangen, Germany, and FDR Visionary Suite and FDR Go; Fujifilm, Tokyo, Japan). All radiographs were acquired using frontal projections (posteroanterior views for patients who were able to stand, and anteroposterior views for portable studies and patients who could not stand).

Initial and follow-up frontal CXR of the patients with confirmed COVID-19 were included for review. The DICOM (digital imaging and communications in medicine) images were anonymised and reviewed by three fellowship/subspeciality-trained thoracic radiologists with 12, 15 and 17 years of experience, respectively, using a 2,048 × 2,048 pixel monitor (Barco, Sunnyvale, CA, USA). For patients with multiple follow-up CXR, the radiographs were systematically reviewed by the three readers to select the radiograph deemed to have the worst findings for analysis. These radiographs were reviewed independently and the final decision was reached by consensus. The reviewers were blinded from the clinical findings of the patients.

Radiographs were assessed for the presence, predominant pattern and distribution of lung parenchymal abnormalities. The CXR were analysed and categorised as either normal or abnormal.

If abnormal, the dominant pattern of lung parenchymal abnormality was assessed, the extent of involvement was recorded as unifocal, unilateral multifocal or bilateral multifocal, and their distribution was then categorised as predominant central, peripheral or mixed.

Each lung field was divided into three zones: upper, middle or lower zones, with each zone spanning one-third of the craniocaudal distance of the lung field. An opacity was considered central if most of the abnormality was located within the medial two-thirds of the lung, and peripheral if most of it was located within the lateral one-third of the lung. The patterns of the lung parenchymal abnormalities were categorised as: consolidation (homogeneous opacification of parenchyma with obscuration of vessels); ground-glass (hazy opacification without obscuring vessels); nodular opacities (focal round opacities); or reticular opacities (linear opacities that form a mesh-like pattern). We also recorded the presence of any other associated findings such as pleural effusion, cavitation, lymphadenopathy and pneumothorax.

RESULTS

There were 52 men and 44 women in the study group (mean age 46.2 ± 14.2 years; age range 16–79 years; Table I). 93.4% of patients were initially seen at the National Centre for Infectious Diseases, the centralised national facility designated for managing the outbreak. The majority of patients were of Chinese ethnicity, accounting for 86.5% (83/96) of the cohort. Out of the 96 patients, 8 (8.3%) had underlying diabetes mellitus and 10 (10.4%) had hypertension. The mean duration from onset of symptoms to admission was 5.7 ± 6.3 days.

In total, we reviewed 347 CXR performed on 96 patients (mean CXR 3.6 ± 3.9; range 1–32 per patient). Mean duration from initial CXR to the follow-up CXR that was deemed to have the worst findings was 8.2 ± 9.8 days. Only one patient who required mechanical ventilation

developed superimposed *Klebsiella* pneumonia. Mean duration from onset of symptoms for the 55 patients who presented with normal CXR at presentation was 5.9 ± 7.5 days. Of the 55 patients with normal initial CXR, 16 (29.1%) did not require follow-up radiographs because of clinical improvement. Of the remaining 39 (70.9%) patients, 13 (33.3%) subsequently showed abnormal CXR findings, with a slight majority presenting predominantly with ground-glass opacities.

Table I. Summary of patient characteristics (n = 96).

Characteristic	No. (%)
Gender	
Men	52 (54.2)
Women	44 (45.8)
Age* (yr)	46.2 ± 14.2 (16–79)
Ethnicity	
Chinese	83 (86.5)
Bangladeshi	5 (5.2)
Indian	2 (2.1)
Malay	1 (1.0)
Others	5 (5.2)
Comorbidity	
Hypertension	10 (10.4)
Diabetes mellitus	8 (8.3)
Underlying pulmonary condition	2 (2.1)

**Data presented as mean ± standard deviation (range).*

At the initial presentation, 41 of the 96 patients (42.7%) had abnormal CXR (Table II). The mean duration from onset of symptoms for patients who presented with abnormal CXR at initial presentation was 5.3 ± 4.7 days. The predominant pattern of lung parenchymal abnormality was ground-glass opacity on initial radiograph, and this was seen in 21 (51.2%) patients. 12 (29.3%) patients had unifocal lesions on initial presentation (Fig. 1). There was a predilection for involvement of the lower zones, as seen in 37 (90.2%) patients. Right lung involvement was more common than the left (34/41, 82.9% vs. 32/41, 78.0%; Table III).

Table II. Abnormal radiographic findings of COVID-19 pneumonia at initial presentation and follow-up.

Radiographic feature	No. (%)	
	Initial presentation (n = 41)	Follow-up (n = 49)
Predominant pattern		
Consolidation	19 (46.3)	25 (51.0)
Ground-glass	21 (51.2)	24 (49.0)
Nodular opacities	1 (2.4)	0 (0)
Reticular opacities	0 (0)	0 (0)
Lesions		
Unifocal	12 (29.3)	15 (30.6)
Multifocal unilateral	3 (7.3)	5 (10.2)
Multifocal bilateral	26 (63.4)	29 (59.2)
Distribution		
Central	6 (14.6)	6 (12.2)
Peripheral	8 (19.5)	8 (16.3)
Mixed	27 (65.9)	35 (71.4)

Abnormal follow-up radiographs refer to radiographs deemed to have the worse findings. Mean duration ± standard deviation from initial to follow-up radiograph was 8.2 days ± 9.8 days.

Table III. Location of lung parenchymal abnormalities in COVID-19 pneumonia on initial and follow-up chest radiographs.

Lung zone	Initial presentation (n = 41)			Follow-up (n = 49)		
	Right lung	Left lung	Right and/or left lung	Right lung	Left lung	Right and/or left lung
Upper	13 (31.7)	6 (14.6)	13 (31.7)	20 (40.8)	14 (28.6)	20 (40.8)
Middle	21 (51.2)	25 (61.0)	28 (68.3)	26 (53.1)	28 (57.1)	32 (65.3)
Lower	30 (73.2)	28 (68.3)	37 (90.2)	39 (79.6)	32 (65.3)	46 (93.9)
Laterality	34 (82.9)	32 (78.0)	–	42 (85.7)	36 (73.5)	–

Abnormal follow-up radiographs refer to radiographs deemed to have the worse findings. Mean duration ± standard deviation from initial to follow-up radiograph was 8.2 days ± 9.8 days. Data is presented as no. (%) of patients.

In follow-up radiographs that were deemed abnormal (n = 49), consolidation was the predominant pattern, as seen in 25 of the 49 patients (51.0%; Table II, Figs. 2 & 3). A majority of the lesions were multifocal and bilateral, and this was seen in 26 of 41 patients (63.4%) and 29 of 49 patients (59.2%) at initial presentation and follow-up, respectively. Mixed central and peripheral distribution of the lung parenchymal abnormalities was more common than central distribution; on follow-up, 71.4% of the radiographs showed mixed central and peripheral

distribution as opposed to 16.3% with peripheral distribution. A predilection for the lower zones was also observed at follow-up, as seen in 46 of the 49 patients (93.9%; Table III). On follow-up, right lung involvement was more common than the left (42/49. 85.7% vs. 36/49, 73.5%). Unilateral pleural effusion was seen in only one patient. No other features such as cavitation, lymphadenopathy or pneumothorax were detected.

DISCUSSION

In many parts of the world, CXR are commonplace in the management of COVID-19. Better understanding of CXR features in this disease would enable appropriate use for triaging and treatment evaluation. At present, publications on chest CT in COVID-19 outnumber those on CXR.

From our experience, the advantage of detecting subtle pulmonary involvement not depicted on CXR can be outweighed by the logistical challenges of transferring patients out of their isolation rooms into the radiology department for CT and the potential risk of disease transmission to healthcare workers and other patients. Furthermore, we have observed that subsequent serial radiographs helps to detect progression of pulmonary involvement without compromising patient care. In a retrospective review of 21 patients by Chung et al, 18 (85.7%) patients had abnormalities on the initial chest CT studies.[13] In a larger study of 138 patients, all patients had positive chest CT with bilateral distribution of lung parenchymal abnormalities.[14] Chest CT may be utilised in a setting where urgent detection and diagnosis of COVID-19 infection is required while awaiting results from respiratory samples, although this would depend on the pre-test probability of COVID-19. For these reasons, we do not recommend CT as an initial diagnostic test. This is in line with the recent recommendations by the American College of

Radiology and the British Society of Thoracic Imaging, which state that CT should be utilised for specific clinical indications, and not be used to screen for COVID-19 or as a first-line test to diagnose COVID-19.[15,16] A recently published consensus statement from the Fleischner Society recommends imaging for patients with mild symptoms who are at risk of disease progression, patients with moderate to severe features, and those with worsening respiratory status.[17] We have therefore sought to methodically study the CXR findings in our initial national cohort of patients.

In this retrospective study of the initial 96 confirmed cases of COVID-19 in Singapore, 55 (57.3%) patients were found to have normal initial CXR. This is higher compared to Wong et al's study, where 31% of the 64 patients had normal initial CXR,[18] and as quoted in the review by Hosseiny et al.[19] This discrepancy could be attributed to aggressive contact tracing as a disease containment strategy in Singapore, resulting in early detection and isolation of symptomatic COVID-19 patients. It is also lower than the reported incidence of abnormal CT findings.[20] Still, it is not unexpected given the higher sensitivity of CT for lung disease, particularly the ground-glass changes that predominate in COVID-19. We believe that our reported incidence rate of abnormal CXR better reflects the spectrum of COVID-19 infections.

In our series, the middle and lower lung zones were predominantly involved, alluding to dominant lower lobe disease. These findings concur with recent publications on CT findings of COVID-19 pneumonia, which showed that multifocal bilateral lung involvement – worse in the lower lobes – was the predominant abnormality.[13,21-24] Similarly, a preliminary study on the ultrasonography findings of COVID-19 pneumonia found that the posterior lungs, particularly in the lower lung fields, were commonly involved.[25]

In our analysis, combined central and peripheral involvement was more common, unlike recent publications on COVID-19, which reported that peripheral distribution was more commonly

observed on CT[13,21-24] and CXR.[18,19] A plausible explanation for the greater central radiographic distribution of consolidation in our series is the summation effect of the abnormalities that are located posteriorly and medially in the lower lobes on 2D analysis, which although peripheral in distribution on CT, may be projected as central, i.e. close to the hilum on CXR, as demonstrated in Fig. 4. Another factor could be our definition of peripheral involvement as the outer 1/3 of the lung field, which takes into account the curved anatomy of the thorax, and the greater volume of the periphery based on prior publications on CT findings of SARS and MERS.[26,27] The study by Wong et al defined peripheral involvement as the lateral half,[18] while the review by Hosseiny et al was an extrapolation from CT findings.[19] We opine that direct analysis of radiographic features of this novel infection – rather than based on extrapolation from CT – is vital, as the two modalities differ in their sensitivity for depicting the pattern and location of lung disease.

Based on our findings, the predominant pattern of lung parenchymal abnormality was that of ground-glass opacity (51.2%) on initial presentation. This is in line with the published literature, which reported ground-glass opacities, mixed ground-glass opacities and consolidation as the predominant lung parenchymal abnormalities on CT.[13,21-24] Our results showed an almost equal proportion of ground-glass opacity and consolidation in both the initial and follow-up radiographs, with a slight predominance for ground-glass opacity. It is known that CT has higher sensitivity for detecting mild ground-glass opacities compared to CXR. However, it is not known if the detection of such mild ground-glass opacities necessarily portends a poorer prognosis. Conversely, patients with more severe disease requiring extended hospitalisation have been found to have a greater prevalence of consolidation, which can readily be appreciated on CXR.[28]

The imaging features of COVID-19 have been compared with those of SARS and MERS. The review by Hosseiny et al has highlighted the overlapping radiographic features of the three human coronavirus infections, but this was based on extrapolation of reports from CT images of COVID-19.[19] Nonetheless, our study confirms that ground-glass opacity and consolidation predominate in the lower lobe and posterior lungs in COVID-19.

Table IV. Predominant initial radiographic findings in coronavirus disease 2019 (COVID-19) pneumonia, severe acute respiratory syndrome (SARS) and Middle East respiratory syndrome (MERS).

Findings	COVID-19 (n = 96)	SARS (n = 138)[29]	MERS (n = 55)[31]
Predominant pattern	Ground-glass opacity: 51.2%	Consolidation: 78.3%	Ground-glass opacity: 66%
Lesion location	Multifocal bilateral: 63.4%	Unifocal: 54.6%	Unifocal: 69%
Distribution	Mixed: 65.9%	Peripheral: 75.0%	Peripheral: 58%
Lung zones			
Middle zone	68.3%	52.8%	54.5%
Lower zone	90.2%	64.8%	69.1%
Laterality			
Right	82.9%	75.9%	85.5%
Left	78.0%	62.0%	63.6%

In a retrospective review of 138 patients with SARS in Hong Kong, Wong et al reported that 78.3% of patients had airspace opacities with ill-defined margins, which obscured the vasculature compatible with consolidation. The involved lung zones were predominantly middle (52.8%) and lower (64.8%) with peripheral location (75%) on initial radiographs.[29] Our findings showed a slight predominance of ground-glass opacity on initial radiographs, and this was the most common parenchymal abnormality in a predominantly mid- and lower-zone distribution. However, unifocal distribution was more common in SARS,[29,30] in contrast to multifocal bilateral lung involvement seen in 63.4% of our patients. We illustrate this difference with two cases from our local institution who were diagnosed with SARS in 2003; one of them developed multifocal

peripheral consolidation, while the other had unifocal consolidation (Fig. 5). MERS appeared to show similar location and distribution of lung involvement, which were unifocal and peripheral, respectively.[31] However, the predominant pattern of abnormality was reported to be ground-glass opacification in contrast to SARS (Fig. 6, Table IV).

Chung et al reported that ground-glass opacities were more common on CT, as seen in 12 out of 21 patients (57%) with COVID-19 pneumonia, while consolidation with ground-glass opacities was seen in 6 out of 21 patients (29%).[13] It was also reported that a peripheral location of opacities was common (33%).[13] Both Chung et al and Huang et al reported that multifocal bilateral lung involvement was a commonly seen pattern.[11,13] Ground-glass opacities and consolidation in subpleural regions were the predominant early CT findings in SARS, while extensive ground-glass opacities and consolidation in basilar and subpleural distributions were common in MERS.[26,27] On CT, multifocal bilateral involvement has been more commonly observed in COVID-19 pneumonia and MERS, as opposed to unifocal involvement in SARS,[11,13,26,27] although this may be confounded by the more widespread use of CT in the current pandemic.

Viral pneumonia has a variable appearance on CXR and CT. Moreover, co-infection with a bacterial pathogen or inflammatory lung disease often confounds radiologic findings. Nevertheless, most viral pneumonia patterns exhibit similarities on the basis of viral families or viridae, as they share similar pathogenic mechanisms.[3] The finding of multifocal bilateral lung consolidation may overlap with other infective pneumonia and may therefore be difficult to distinguish on imaging. Viral pneumonia of adenovirus, herpes simplex virus and bocavirus aetiology are known to cause multifocal or diffuse bilateral lung consolidation, while cytomegalovirus pneumonia may show bilateral ground-glass opacities and airspace

consolidation.[3] On CXR, influenza pneumonia typically demonstrates bilateral reticulonodular opacities with or without consolidation and predominantly involves the lower lobes; on CT, they commonly show centrilobular nodules in peripheral distribution, although ground-glass opacities and consolidation have also been described.[3,32,33] Bacterial pneumonias mainly show lobar or broncho-pneumonia and present as extensive patchy consolidations of lung parenchyma on CT, while mycoplasma pneumonia manifests as bronchial wall-thickening and centrilobular nodules.[34]

SARS-CoV-2 has been described to invade the bronchioles, causing bronchiolitis and peribronchitis with subsequent distal spread, thus giving rise to initial ground-glass opacity and subsequent lobular patchy opacity when the entire secondary pulmonary lobule is involved.[35] In addition, further involvement of the interlobular interstitium results in the 'fine reticulation' sign.[35] Variable findings COVID-19 pneumonia, depending on the time course of the disease at which the imaging is taken, may pose a diagnostic challenge to radiologists. Ground-glass opacities found on initial CT were shown to progress to consolidation during the peak stage of the disease (9–13 days from onset of symptoms) before showing interval improvement after 14 days.[36] In our study, the mean duration from onset of symptoms to an abnormal CXR finding was 5.3 days. Hence, the interpretation of radiographic and CT findings in a suspected or confirmed case should be correlated with the duration of symptom onset to improve diagnostic performance.

This retrospective study is limited by a lack of correlation with patient symptoms and long-term outcome. Nevertheless, our observations of certain predominant radiographic patterns are informative in dealing with this novel respiratory tract infection, and we have also highlighted specific key differences in findings from recent publications on CXR features of COVID-19, which have been mainly limited to describing chest CT. As the current pandemic continues to

evolve, we expect to better determine the natural progression of radiographic findings in relation to novel treatment regimens such as the use of anti-retroviral medications (e.g. combination of lopinavir and ritonavir).[11]

In conclusion, CXR is widely used as a tool for prompt initial evaluation and subsequent management of COVID-19 pneumonia. However, its imaging features have not been as well-described as those for chest CT. We found the incidence of abnormal CXR on presentation to be lower and mixed central and peripheral involvement to be more common than previously reported. Improved understanding of the patterns of radiographic findings will enhance diagnostic workflow and the appropriate use of CXR in public health measures to deal with the current pandemic.

ACKNOWLEDGEMENT

Recruitment of study participants and sample collection was funded by a seed grant from the Singapore National Medical Research Council (TR19NMR119SD; project reference number: CCGSFPOR20001).

REFERENCES

1. Weiss SR, Leibowitz JL. Coronavirus pathogenesis. Adv Virus Res 2011; 81:85-164.
2. Galante O, Avni YS, Fuchs L, Ferster OA, Almog Y. Coronavirus NL63-induced adult respiratory distress syndrome. Am J Respir Crit Care Med 2016; 193:100-1.
3. Koo HJ, Lim S, Choe J, et al. Radiographic and CT features of viral pneumonia. Radiographics 2018; 38:719-39.

4. World Health Organization. Summary of probable SARS cases with onset of illness from 1 November 2002 to 31 July 2003. Available at: https://www.who.int/csr/sars/country/table2004_04_21/en/. Accessed April 29, 2020.
5. World Health Organization. Middle East respiratory syndrome coronavirus (MERS-CoV). Available at: https://www.who.int/emergencies/mers-cov/en/. Accessed April 29, 2020.
6. Zhu N, Zhang D, Wang W, et al. A novel coronavirus from patients with pneumonia in China, 2019. N Engl J Med 2020; 382:727-33.
7. World Health Organization. Novel coronavirus (2019-nCoV) situation report – 1. 21 January 2020. Available at: https://www.who.int/docs/default-source/coronaviruse/situation-reports/20200121-sitrep-1-2019-ncov.pdf?sfvrsn=20a99c10_4. Accessed April 29, 2020.
8. Guarner J. Three emerging coronaviruses in two decades. Am J Clin Pathol 2020; 153:420-1.
9. World Health Organization. WHO Director-General's opening remarks at the media briefing on COVID-19 – 11 March 2020. Available at: https://www.who.int/dg/speeches/detail/who-director-general-s-opening-remarks-at-the-media-briefing-on-covid-19---11-march-2020. Accessed April 29, 2020.
10. Ng MY, Lee EY, Yang J, et al. Imaging profile of the COVID-19 infection: radiologic findings and literature review. Radiology: Cardiothoracic Imaging 2020; 2:e200034.
11. Huang C, Wang Y, Li X, et al. Clinical features of patients infected with 2019 novel coronavirus in Wuhan, China. Lancet 2020; 395:497-506.
12. Chen N, Zhou M, Dong X, et al. Epidemiological and clinical characteristics of 99 cases of 2019 novel coronavirus pneumonia in Wuhan, China: a descriptive study. Lancet 2020; 395:507-13.

13. Chung M, Bernheim A, Mei X, et al. CT imaging features of 2019 novel coronavirus (2019-nCoV). Radiology 2020; 295:202-7.
14. Wang D, Hu B, Hu C, et al. Clinical characteristics of 138 hospitalized patients with 2019 novel coronavirus-infected pneumonia in Wuhan, China. JAMA 2020; 323:1061-9.
15. American College of Radiology. ACR Recommendations for the use of chest radiography and computed tomography (CT) for suspected COVID-19 infection. Available at: https://www.acr.org/Advocacy-and-Economics/ACR-Position-Statements/Recommendations-for-Chest-Radiography-and-CT-for-Suspected-COVID19-Infection. Accessed April 29, 2020.
16. British Society of Thoracic Imaging. COVID-19 BSTI statement and guidance. Available at: https://www.bsti.org.uk/standards-clinical-guidelines/clinical-guidelines/covid-19-bsti-statement-and-guidance/. Accessed April 29, 2020.
17. Rubin GD, Ryerson CJ, Haramati LB, et al. The role of chest imaging in patient management during the COVID-19 pandemic: a multinational consensus statement from the Fleischner Society. Radiology 2020; 296:172-80.
18. Wong HYF, Lam HYS, Fong AHT, et al. Frequency and distribution of chest radiographic findings in patients positive for COVID-19. Radiology 2020; 296:E72-8.
19. Hosseiny M, Kooraki S, Gholamrezanezhad A, Reddy S, Myers L. Radiology perspective of coronavirus disease 2019 (COVID-19): lessons from severe acute respiratory syndrome and Middle East respiratory syndrome. AJR Am J Roentgenol 2020; 214:1078-82.
20. Ai T, Yang Z, Hou H, et al. Correlation of chest CT and RT-PCR testing for coronavirus disease 2019 (COVID-19) in China: a report of 1014 cases. Radiology 2020; 296:E32-40.

21. Bernheim A, Mei X, Huang M, et al. Chest CT findings in coronavirus disease-19 (COVID-19): relationship to duration of infection. Radiology 2020; 295:200463.
22. Zhou S, Wang Y, Zhu T, Xia L. CT features of coronavirus disease 2019 (COVID-19) pneumonia in 62 patients in Wuhan, China. AJR Am J Roentgenol 2020; 214:1287-1294.
23. Zhao W, Zhong Z, Xie X, Yu Q, Liu J. Relation between chest CT findings and clinical conditions of coronavirus disease (COVID-19) pneumonia: a multicenter study. AJR Am J Roentgenol 2020; 214:1072-7.
24. Zu ZY, Jiang MD, Xu PP, et al. Coronavirus disease 2019 (COVID-19): a perspective from China. Radiology 2020; 296:E15-25.
25. Huang Y, Wang S, Liu YL, et al. A preliminary study on the ultrasonic manifestations of peripulmonary lesions of noncritical novel coronavirus pneumonia (COVID-19). Research Square 2020. https://doi.org/10.21203/rs.2.24369/v1. Preprint.
26. Ajlan AM, Ahyad RA, Jamjoom LG, Alharthy A, Madani TA. Middle East respiratory syndrome coronavirus (MERS-CoV) infection: chest CT findings. AJR Am J Roentgenol 2014; 203(4):782-7.
27. Ooi GC, Khong PL, Müller NL, et al. Severe acute respiratory syndrome: temporal lung changes at thin-section CT in 30 patients. Radiology 2004; 230:836-44.
28. Shi H, Han X, Jiang N, et al. Radiological findings from 81 patients with COVID-19 pneumonia in Wuhan, China: a descriptive study. Lancet Infect Dis 2020; 20:425-34.
29. Wong KT, Antonio GE, Hui DSC, et al. Severe acute respiratory syndrome: radiographic appearances and pattern of progression in 138 patients. Radiology 2003; 228:401-6.
30. Paul NS, Roberts H, Butany J, et al. Radiologic pattern of disease in patients with severe acute respiratory syndrome: the Toronto experience. Radiographics 2004; 24:553-63.

31. Das KM, Lee EY, Al Jawder SE, et al. Acute Middle East respiratory syndrome coronavirus: temporal lung changes observed on the chest radiographs of 55 patients. AJR Am J Roentgenol 2015; 205:W267-74.
32. Kloth C, Forler S, Gatidis S, et al. Comparison of chest-CT findings of influenza virus-associated pneumonia in immunocompetent vs. immunocompromised patients. Eur J Radiol 2015; 84:1177-83.
33. Franquet T. Imaging of pulmonary viral pneumonia. Radiology 2011; 260:18-39.
34. Dai WC, Zhang HW, Yu J, et al. CT imaging and differential diagnosis of COVID-19. Can Assoc Radiol J 2020; 71:195-200.
35. Meng H, Xiong R, He R, et al. CT imaging and clinical course of asymptomatic cases with COVID-19 pneumonia at admission in Wuhan, China. J Infect 2020; 81:e33-9.
36. Pan F, Ye T, Sun P, et al. Time course of lung changes on chest CT during recovery from coronavirus disease (COVID-19). Radiology 2020; 295:715-21.

FIGURES

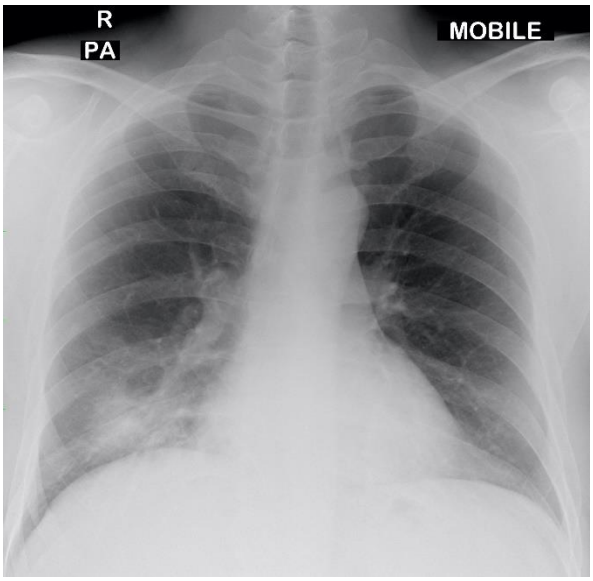

Fig. 1 A 35-year-old man with fever and cough for one day. Chest radiograph obtained at Day 1 of symptoms shows a unifocal consolidation in the right lower zone, predominantly in the infrahilar location.

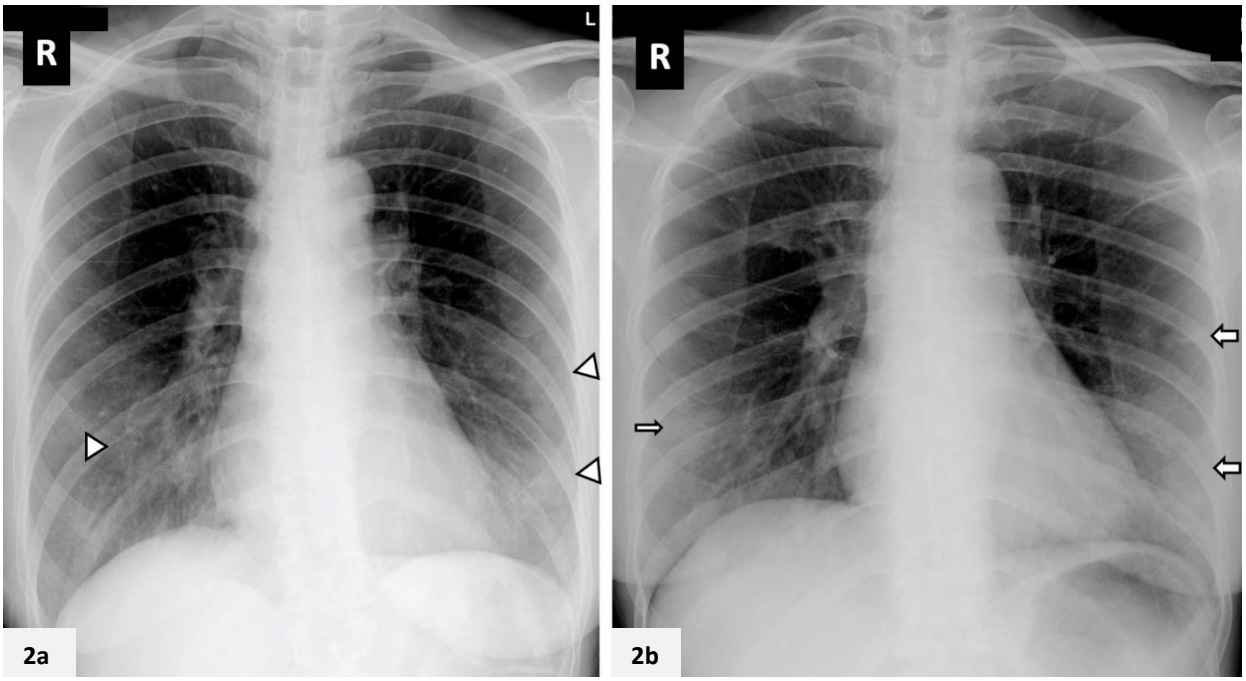

Fig. 2 A 55-year-old woman with fever, cough and dyspnoea for 4 days. (a) Initial chest radiograph obtained on Day 4 of symptoms shows multifocal ground-glass opacities in the bilateral lower zones (arrowheads). (b) Follow-up radiograph performed 2 days later shows increased density in the left lower zone (broad arrows), in keeping with consolidation. A small focus of consolidation is also seen in the right lower zone (thin arrow).

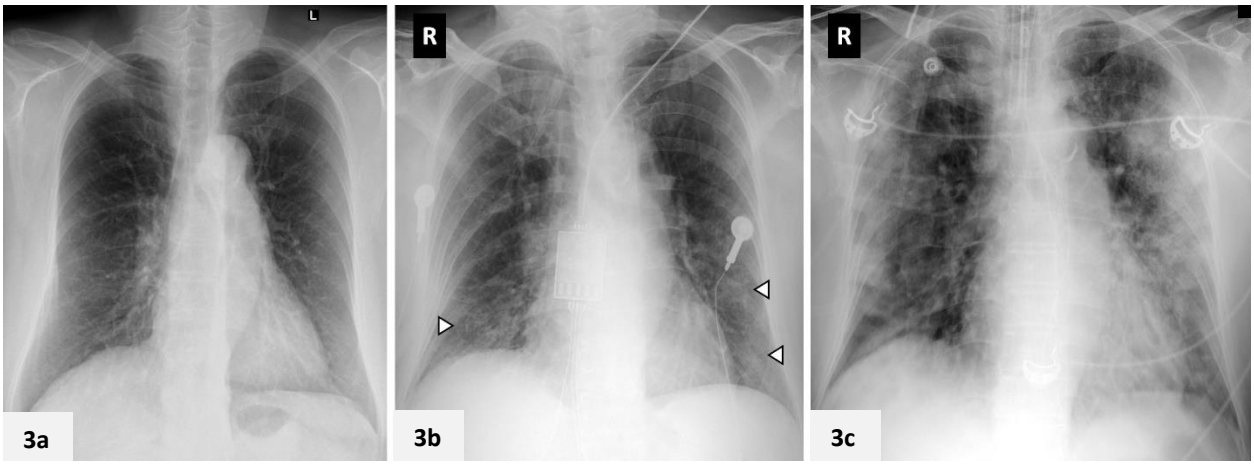

Fig. 3 A 77-year-old woman with fever, cough and sore throat for 5 days. (a) Initial chest radiograph on admission is normal. (b) Follow-up radiograph performed 2 days later shows interval development of multifocal ground-glass opacities in the bilateral lower zones (arrowheads). The patient deteriorated during admission and required intensive care admission for mechanical ventilation. (c) Radiograph obtained on Day 11 of admission shows progression of lung changes with multifocal bilateral lung consolidation, worse in the left lung.

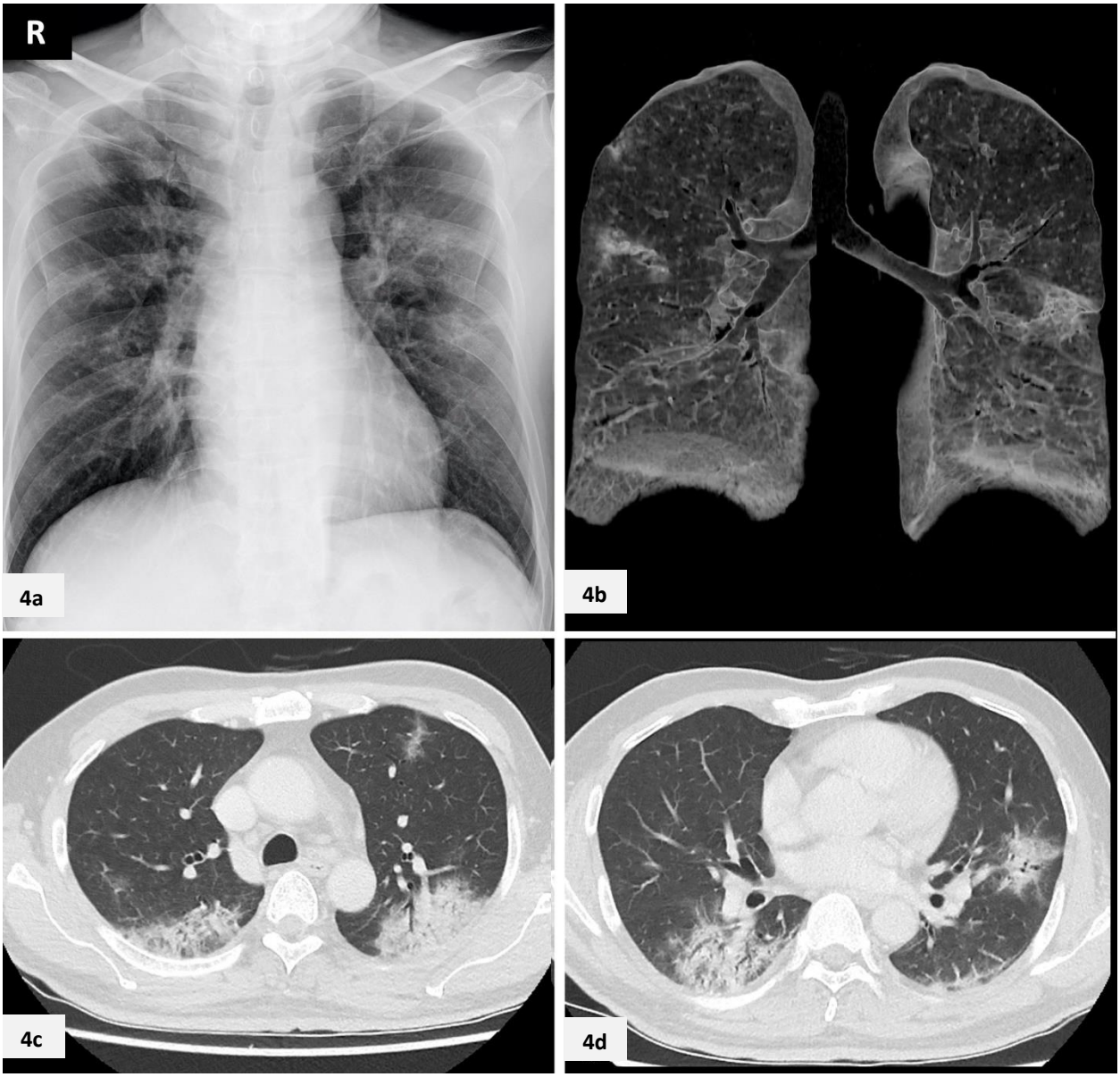

Fig. 4 A 56-year-old man with a travel history to China who presented with cough and sputum production. Imaging studies were all obtained on Day 12 after the onset of symptoms. (a) Chest radiograph shows multifocal bilateral lung consolidation, involving all three zones of the right lung as well as the left upper and middle zones. (b) Volume-rendered maximum intensity projection 3D CT image shows the pattern of lung involvement, which is predominantly peripheral in location, involving the posterior and dependent areas of the lungs. (c & d) Axial contrast-enhanced CT images in lung window show multifocal confluent areas of consolidation that are extended to the subpleural and peripheral locations. Note the patchy scattered pure ground-glass opacities, and the absence of nodules and reticular opacities; these were not evident on chest radiograph. There is an absence of both thoracic nodal enlargement and pleural effusion.

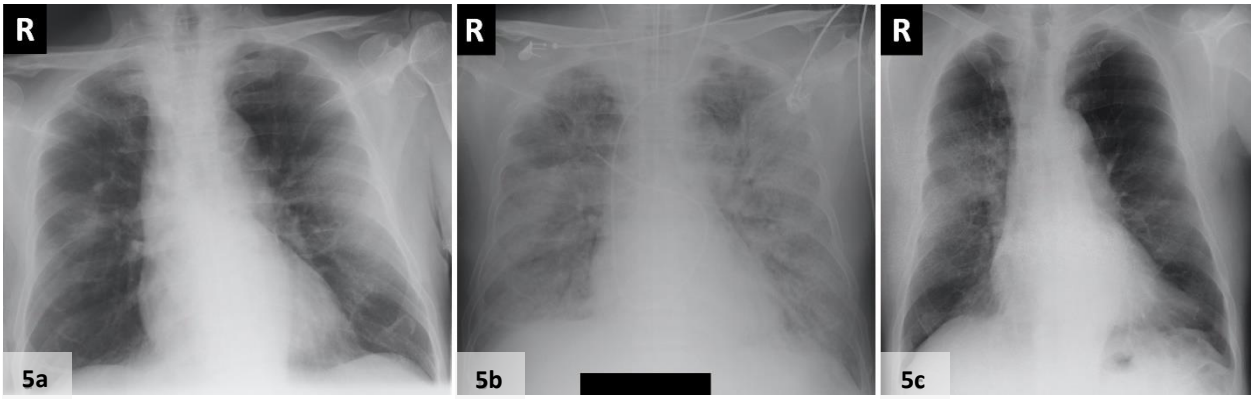

Fig. 5 (a & b) A 72-year-old woman diagnosed with SARS in 2003. (a) Initial chest radiograph obtained on Day 5 of symptoms shows bilateral lung consolidation in the right middle as well as left middle and lower zones, which appear predominantly peripheral in location. (b) Follow-up radiograph performed 13 days later shows worsening lung changes with diffuse bilateral lung consolidation, in keeping with the picture of acute respiratory distress syndrome. The patient succumbed to the disease one day later despite intensive care support. (c) A 68-year-old man with SARS admitted in 2003. Chest radiograph taken on Day 6 of symptoms shows a focus of unifocal ill-defined consolidation with concomitant reticular markings in the right middle zone. The patient was discharged well after 2 weeks.

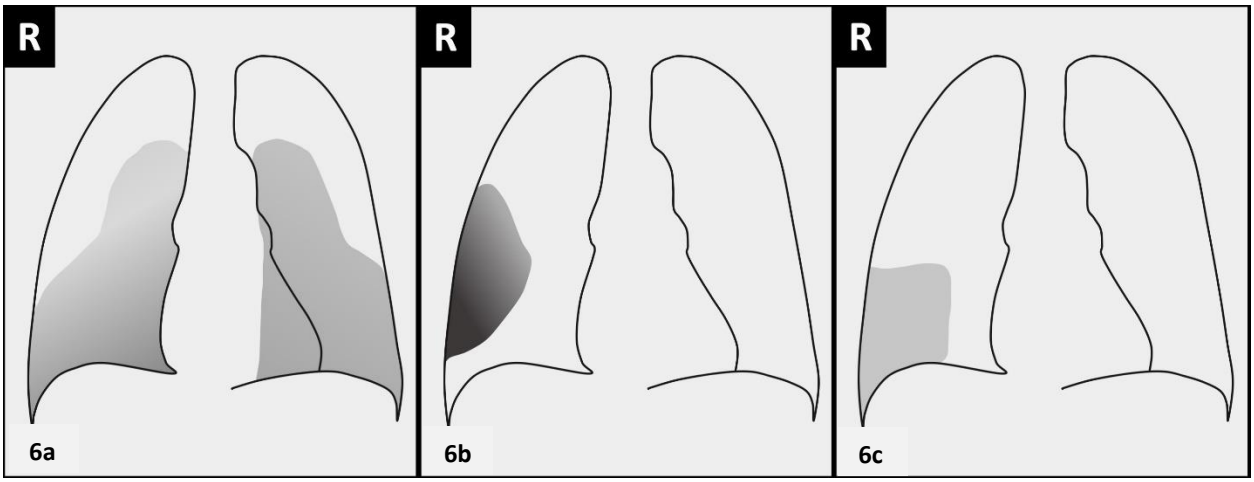

Fig. 6 Chest radiograph illustrations of the typical lung parenchymal abnormality and distribution in (a) COVID-19 pneumonia – multifocal bilateral lung ground-glass opacities in mixed central and peripheral distribution; (b) SARS – unifocal right lung consolidation, predominantly in peripheral distribution; and (c) MERS – unilateral ground-glass opacity in the peripheral location.